

---

# Quantifying the Preferential Direction of the Model Gradient in Adversarial Training With Projected Gradient Descent

---

**Ricardo Bigolin Lanfredi**

Scientific Computing and Imaging Institute  
University of Utah  
Salt Lake City UT 84112  
ricbl@sci.utah.edu

**Joyce D. Schroeder**

Department of Radiology and Imaging Sciences  
University of Utah  
Salt Lake City UT 84112  
joyce.schroeder@hsc.utah.edu

**Tolga Tasdizen**

Scientific Computing and Imaging Institute  
University of Utah  
Salt Lake City UT 84112  
tolga@sci.utah.edu

## Abstract

Adversarial training, especially projected gradient descent (PGD), has been the most successful approach for improving robustness against adversarial attacks. After adversarial training, gradients of models with respect to their inputs are meaningful and interpretable by humans. However, the concept of interpretability is not mathematically well established, making it difficult to evaluate it quantitatively. We define interpretability as the alignment of the model gradient with the vector pointing toward the closest point of the support of the other class. We propose a method for measuring this alignment for binary classification problems, using generative adversarial model training to produce the smallest residual needed to change the class present in the image. We show that PGD-trained models are more interpretable than the baseline according to our definition, and our metric presents higher alignment values than a competing metric formulation. We also show that enforcing this alignment increases the robustness of models without adversarial training.

## 1 Introduction

Deep learning models have been shown to suffer from a lack of robustness against directed attacks that produce only small perturbations to the original input [12]. Several attacks of varying strengths have been proposed [36]. To solve the problem of lack of robustness, researchers have proposed several methods for defending against such attacks [36]. These defenses include, for instance, training using adversarial examples as samples [12, 26], preprocessing input data [13], regularizing gradients [30, 25, 18, 15], and detecting adversarial attacks [3]. One of the most successful defenses in terms of resisting new attacks [2, 4] is projected gradient descent (PGD) training [26]. When applying this method, adversarial examples are found using iterative optimization with projection to a constrained space after each iteration, and the resulting modified input is used for training.

PGD has been shown to make  $\nabla_{L(x)}$ , the gradient of the loss function of a trained model with respect to inputs  $x$ , more interpretable [33]. Other robust training techniques also induce interpretable models [20, 8, 35, 21]. We focus our studies on PGD with an  $L^\infty$  constraint due to its success and

widespread use [26, 2, 4]. There is no single way of mathematically establishing the concept of increased interpretability of  $\nabla_{L(x)}$ , and only a few quantitative studies have related gradient direction to robustness. We propose a novel definition for this concept in binary classification datasets. We formulate a gradient alignment  $\alpha_{\Delta x}$  for a given sample  $x$  as the cosine similarity between  $\nabla_{L(x)}$  and a vector  $\Delta x$  pointing from  $x$  to its closest point  $x'$  in the support of the opposite class. We call the direction of this vector as the interpretable direction. This definition is not the only way of defining interpretability, but it is intuitively related to it.

We start by analyzing the robustness of models in a toy dataset where the data for each class lies in one of two concentric spheres, inspired by the work of Gilmer et al. [10]. The dataset was used by Gilmer et al. [10] to demonstrate that non-zero generalization error can be the only cause of adversarial examples. We, nonetheless, use the dataset to prove a proportional relation between robustness and the proposed alignment metric. The theorems used for this proof are generic for binary classification problems, assuming local linearity and specific characteristics of the data distribution. Since  $x'$  is not straightforward to calculate for complex datasets, we also proposed a method to calculate an approximation  $\hat{x}'$ . This method draws from the method visualization for regression with a generative adversarial network (VR-GAN)[23], which uses generative adversarial training [11] to train a generator to produce difference maps that, when added to an input sample, change its associated label. We proceed to evaluate if the metric provides information for more complex datasets. Our results show that the most robust model did not always match the model with closer alignment, showing that the metric is not a direct representation of model robustness. However, we show that the metric is informative, since, compared to a baseline, robust models trained with PGD have a larger  $\alpha_{\Delta x}$ , and models trained using  $\alpha_{\Delta x}$  for enforcing a penalty on its gradient have higher robustness. Furthermore, models show a closer alignment to the proposed metric than an existing alignment metric proposed by Etmann et al. [8].

## 1.1 Related work

Etmann et al. [8] mathematically defined the alignment of gradients after robust training as the alignment between the input image and the model gradient. Robustness is shown to be bounded by the sum of the given metric with other terms related to gradients and internal bias weights. We argue that this definition is not intuitive since an interpretable saliency map should not necessarily highlight the whole input sample nor be directly proportional to the inputs. We compare the metric proposed by Etmann et al. [8] against our metric and demonstrate that ours presents a closer alignment in practice. In analyses of Ilyas et al. [16] and Tanay and Griffin [32], the gradient of robust models is shown to be more aligned with the vector connecting the centroid of two classes than the gradients of non-robust models. However, this finding is restricted to linear models. The complex boundaries of piecewise linear deep learning models are unlikely to benefit from pointing in a single direction over the entire support of classes in high-dimensional datasets. Using local information of projection to the support of the opposite class, as we propose, is required to get flexible directions for each locally linear region of the model, and, thus, for increasing local robustness.

For studying the alignment of gradients quantitatively, we introduce a metric and propose to demonstrate its correlation with robustness. Other metrics with similar correlation properties have been studied. The local linearity measure (LLM) [28], for which a low value represents high local linearity of models around data points, is inversely correlated with the number of iterations in PGD. The metric was not evaluated directly against robustness, despite its potential. The CLEVER metric [34] uses an estimated extreme value for the Lipschitz constant of the model to calculate a lower bound for robustness without having to perform evaluation attacks. This metric complements ours because it does not evaluate the gradient direction, while ours does not evaluate the gradient magnitude.

We propose a penalty on the direction of  $\nabla_{L(x)}$ . This proposal adds to the literature of gradient penalties for robustness. Regularizing the Lipschitz constant of a model has repeatedly been shown to increase its robustness [30, 25]. This regularization is equivalent to performing double backpropagation [7], i.e., to penalizing the norm of  $\nabla_{L(x)}$ . This penalty, therefore, does not penalize the direction of the gradient. Similar propositions have been made for multi-class setups [18, 15]. The local linearity regularizer (LLR) [28] was proposed and combined with PGD to allow faster training. This penalty is equivalent to enforcing the  $\nabla_{L(x)}$  vector to be constant around data samples, but the penalty enforces no direction. An alignment penalty for  $\nabla_{L(x)}$ , aligning  $\nabla_{L(x)}$  with  $x$  instead of  $\Delta x$ , was proposed by Etmann et al. [8], only as a future work. An analogous penalty was proposed by

Chan et al. [6], using the same motivation of interpretable saliency maps being aligned with  $x$ , which we argue is a non-intuitive constraint. The penalty enforces the gradient of the model to resemble  $x$  through an adversarial loss. The alignment proposed by Noack et al. [27] enforces an  $L^2$  loss on the difference between the gradient of the model and a saliency map of the non-robust model generated through SmoothGrad [31], a visual attribution technique. No theoretical justification for the generation of saliency maps through such a technique was given. The method proposed by Chan et al. [5] transfers robustness from one model trained with PGD to other models by using the gradient of the robust model as reference for an alignment penalty, enforced through an adversarial loss and an  $L^2$  loss on the difference between gradients. This proposed penalty has no interpretability motivation and is based only on the fact that gradient direction is one of the reasons for the robustness of models.

## 2 Approach

### 2.1 Motivation and formulation of alignment metric

The robustness of a binary decision model  $m$  at a specific point  $x$  can be defined as the distance of  $x$  to the closest point where it is misclassified by  $m$ . Formally, we define

$$\rho(x) = \begin{cases} \inf\{\|\delta\|_p : m(x + \delta) \neq m(x)\}, & \text{if } m(x) = y \\ -\inf\{\|\delta\|_p : m(x + \delta) \neq m(x)\}, & \text{if } m(x) \neq y \end{cases}, \quad (1)$$

where  $\rho(x)$  is the robustness of  $m$  against adversarial attacks at point  $x$ , and  $y$  is the ground truth class associated with  $x$ . We set a negative distance for misclassified examples to penalize errors and prevent models with a trivial decision boundary, i.e., one that always assigns the same class, to have infinite expected robustness. For this analysis, we will use the  $L^2$  norm, i.e.,  $p = 2$ .

A closer examination of the *Spheres* dataset proposed by Gilmer et al. [10] can provide insights into how to analyze the robustness of deep learning models against adversarial attacks. We describe the motivation for our method using this dataset because its simplicity allows for a more accessible analysis, while locally linear deep learning models can still partially fail in modeling it. We also use this dataset to hypothesize about another aspect related to robustness: the association between the robustness of a binary decision model and the alignment between its gradient with respect to its inputs and interpretable directions. The *Spheres* dataset is composed of two classes with support on the surface of two hyperspheres, of radius 1.0 and 1.3, one for each class, in a 500-dimensional space. The prior probability for each class is 0.5, and the distribution of samples is uniform on each hypersphere surface. We use the term support of a class  $c$  as defined by  $\text{supp}_c = \{x \in X \mid P(x|y = c) > 0\}$ , where  $X$  is the domain of inputs.

For this dataset, the optimally robust model  $m_p$  has its decision rule defined by

$$c = \begin{cases} 1, & \text{if } \|x\|_2 > t \\ 0, & \text{if } \|x\|_2 < t \end{cases}, t = 1.15. \quad (2)$$

This model has a margin of 0.15 between the decision boundary and any data point. Note that the expected robustness  $\mathbb{E}_{x \sim X} [\rho(x)]$  is the same for all values of  $t$ , and the decision to choose  $t = 1.15$  is based on classification margins. A differentiable decision model can be obtained by defining  $m_p(x) = \sigma(\|x\|_2 - 1.15)$ , where  $\sigma$  is the sigmoid function. This model has radial gradients with respect to the input. This property is maintained, with a possible change to the opposite radial direction, after applying a binary cross-entropy loss. We denote the gradient of the resulting loss  $L$  with respect to inputs  $x$  as  $\nabla_{L(x)}$ . The gradients point toward the origin for class 1 and away from the origin for class 0. We note that the optimally robust model has gradients that point from the support of one class to the closest point  $x'$  of the support of the other class. We denote the vector connecting  $x$  to  $x'$  as  $\Delta x$ . We will proceed to theoretically justify the importance of  $\Delta x$ .

**Lemma 1.** *Let  $l(x) = \sup\{r : \forall v \text{ s.t. } \|x - v\|_2 < r, \exists! w, \exists! b \text{ s.t. } m(v) = \sigma(\langle v, w \rangle + b)\}$ , i.e.  $l(x)$  is the radius of the largest hypersphere around  $x$  where a decision model  $m$  can be defined by a specific linear decision function. Assuming that  $l(x) \geq |\rho(x)|$  for  $m$ , then the logits of  $m$  can be modeled as a linear function, i.e.  $\langle x, w \rangle + b$ , for robustness assessment, resulting in a robustness magnitude in  $x$  given by  $|\rho(x)| = \left| \frac{\langle x, w \rangle + b}{\|w\|_2} \right|$ .*

Lemma 1 follows from Lemma 1 in [8], where it is additionally shown that, empirically, despite  $l(x) \geq |\rho(x)|$  not holding, the linearization can be considered a good approximation. We will refer to models satisfying the assumption in Lemma 1 as being locally linear around  $x$ .

**Theorem 1.** *Let  $\text{sim}(u, v)$  be the alignment between vectors  $u$  and  $v$ , defined by their cosine similarity  $\text{sim}(u, v) = \frac{\langle u, v \rangle}{\|u\|_2 \|v\|_2}$ , and let  $m$  be a binary decision model. For a pair of examples  $x_0$  and  $x_1$  from a binary dataset, of class 0 and 1, respectively, and around which  $m$  is locally linear, the combined robustness  $\rho(x_0) + \rho(x_1)$  of  $m$  is directly proportional to  $\alpha$  according to  $\rho(x_0) + \rho(x_1) = \|x_1 - x_0\|_2 \times \alpha$ , where  $\alpha = \text{sim}(x_1 - x_0, \nabla_{L(x_0)}) = \text{sim}(x_0 - x_1, \nabla_{L(x_1)})$  and  $L(x_i)$  is the binary cross-entropy loss for example  $x_i$ .*

Theorem 1 establishes that, given assumptions of local linearity, the sum of the robustness of two inputs of opposite classes is proportional to the alignment between model gradient and a vector connecting both inputs, and will be part of the Theorem 2. The proof for Theorem 1 is in Section C in the Supplementary Material. We proceed to formulate a global metric to measure the robustness of a given model trained for a binary dataset. Therefore, we define the robustness of a model as the expected robustness with respect to the data distribution.

**Theorem 2.** *Assuming that, for a separable binary dataset, it is possible to define a bijection between the support of both classes  $\text{supp}_0$  and  $\text{supp}_1$  such that, given all bijection pairs  $(x_0, x_1)$ ,  $x_0 \in \text{supp}_0$  and  $x_1 \in \text{supp}_1$ ,*

1.  $P(x_0) = P(x_1)$ ,
2. a binary decision model  $m$  is locally linear around  $x_0$  and  $x_1$ ,

then the expected robustness of  $m$ ,  $\rho_m$ , is related to the average alignment  $\bar{\alpha}$  between the model gradient with respect to inputs and  $\Delta x$  of pairs  $(x_0, x_1)$ , according to

$$\rho_m \geq \frac{\inf(K) \times \bar{\alpha}}{2} \quad \text{and} \quad \bar{\alpha} \geq \frac{2 \times \rho_m}{\sup(K)}, \quad (3)$$

where  $K$  is the set of distances  $\|x_1 - x_0\|_2$  over all pairs  $(x_0, x_1)$ .

Theorem 2 sets bounds for the relationship between the expected robustness of a model and the average alignment between the model’s gradient and vectors connecting inputs of opposite classes. This theorem will be used to define (4) heuristically. The proof for Theorem 2 is given in Section C in the Supplementary Material. The local linearity assumption of Theorem 2 is likely to hold only if the bijection can be established between the closest points of both supports. Therefore, we define a metric using the concept of alignment between  $\nabla_{L(x)}$  and the vector pointing to the closest point of the support of the other class, given by

$$\bar{\alpha}_{\Delta x} = \int P(x) \frac{\langle \Delta x, \nabla_{L(x)} \rangle}{\|\Delta x\|_2 \|\nabla_{L(x)}\|_2} dx, \quad \Delta x = \underset{r}{\text{arginf}} \{ \|r\|_2 : (x + r) \in \text{supp}_j, x \in \text{supp}_i, j \neq i \}. \quad (4)$$

Given that assumptions from Theorem 2 are satisfied for the pairs of closest points between supports of opposite classes of a dataset, the metric defined by (4) will be related to the expected robustness  $\rho_m$  following  $\bar{\alpha}$  in (3). For the *Spheres* dataset, it is possible to establish a bijection as required by Theorem 2 using points of opposite classes along the same radial direction. Since the prior probability of both classes is balanced, and the probability distribution in both supports is uniform,  $P(x_0) = P(x_1)$  holds for any pair of points. Thus, except for a possible violation of the local linearity assumption, Theorem 2 holds for the *Spheres* dataset. Additionally, all distances between closest points are constant, so both bounds can be combined into an equality  $\rho_m = \|\Delta x\|_2 \times \bar{\alpha}_{\Delta x} / 2$ . According to Theorem 2, the optimally robust model  $m_p$  has  $\rho_{m_p} = (0.3 \times 1) / 2 = 0.15$ , which is the expected value. However, the assumptions needed for applying Theorem 2 are unlikely to hold exactly for more complex datasets. We perform empirical analysis to evaluate the alignments of such datasets.

**Interpretability** It has been shown that, for models trained for adversarial robustness employing PGD, the gradient of losses with respect to model inputs, also called saliency maps and represented

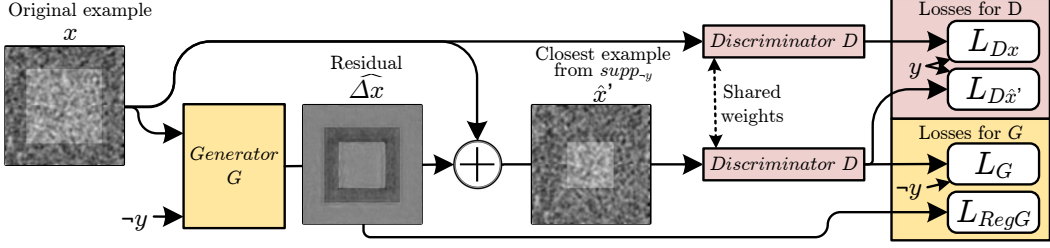


Figure 1: Training diagram for learning to generate residual approximations  $\widehat{\Delta x}$  for complex datasets. The terms  $L_{Dx_0}$ ,  $L_{D\hat{x}_0}$ , and  $L_G$  are classification losses, and  $L_{RegG}$  penalizes the length of  $\widehat{\Delta x}$ .

by  $\nabla_{L(x)}$ , are more interpretable than for models trained with only supervised learning [33]. Etmann et al. [8] studied the relationship between the robustness of a model and the orientation of  $\nabla_{L(x)}$ . However, the proposed alignment metric is measured between  $\nabla_{L(x)}$  and the model input  $x$ . In terms of interpretability, this definition would mean that the whole image, locally modulated by pixel intensity, is being used for the model’s decision. We argue that this definition is a rough approximation of what interpretable alignment should be. For example, if trying to differentiate between images of digits 3 and 5, only the upper part of the number should be used, since the bottom halves of both digits are similar. If the alignment metric is calculated using our metric  $\overline{\alpha_{\Delta x}}$ , only relevant parts of the image will be highlighted, since the interpretable direction will be following the shortest distance between both classes, omitting regions where no change is required.

**Gradient penalty** It has been shown that, in high-dimensional spaces, even models with extremely low generalization error have adversarial regions in the original class supports [10]. This drawback is due to the impracticality of optimizing a model using training examples covering the entire high-dimensional space and causes the model to have regions with incorrect predictions. PGD training partially solves this problem by finding nearby points in the input space that the model misclassifies and using them as training examples. Another method to mitigate this problem is to enforce first-order derivative directions on the loss, providing non-local information and reducing regions with adversarial examples. Additionally, a penalty on the alignment of the gradient will reduce the odds of the gradient pointing in random directions, potentially reducing meaningless changes to the input when performing adversarial attacks. In other words, if  $\nabla_{L(x)}$  is encouraged to point in the direction of the opposite class, adversarial attacks will make more meaningful changes.

We propose that steering  $\nabla_{L(x)}$  by adding a penalty  $L_\alpha$  to a supervised classification loss will increase the robustness of a model. This penalty is given by

$$L_\alpha = -\lambda_\alpha \overline{\alpha_{\Delta x}}, \quad (5)$$

where  $\lambda_\alpha$  is a hyperparameter. This penalty is not meant to replace other robust training methods, but to show that increasing alignment increases robustness.

## 2.2 Generating the alignment vector ground truth

For almost all real-world datasets,  $\Delta x$  is not trivial to find. To generate it, we use generative adversarial training [11] to characterize the support of two classes with a discriminator model  $D$  and to train a conditional generator  $G$  to produce the residuals needed to convert from one class to another. The formulation draws from the VR-GAN [23] method, modified to work with classification tasks instead of regression tasks. Figure 1 shows the overall formulation for the training of the generator. The main objective of this formulation is to find an approximation  $\widehat{\Delta x}$  for the residual  $\Delta x$  pointing from the original example  $x$  of class  $y$  to the closest point  $x'$  in the support of the opposite class  $\neg y$ . This residual is produced according to

$$\hat{x}' = x + \widehat{\Delta x} = x + G(x, \neg y). \quad (6)$$

We set up an adversarial loss given by

$$L_{Dx} = \mathbb{E}[\mathcal{L}(D(x), y)], L_{D\hat{x}'} = \mathbb{E}[\mathcal{L}(D(\hat{x}'), y)], L_G = \mathbb{E}[\mathcal{L}(D(\hat{x}'), \neg y)], \quad (7)$$

where  $\mathcal{L}$  is a classification loss, binary cross-entropy in this particular case,  $L_{Dx}$  and  $L_{D\hat{x}'}$  are losses for which  $D$  is optimized, and  $L_G$  is a loss for which  $G$  is optimized. The generator  $G$  is trained to fool  $D$  ( $L_G$ ), whereas  $D$  is trained not to be fooled ( $L_{D\hat{x}'}$ ). This adversarial setup, combined with a traditional supervised loss ( $L_{Dx}$ ), should make  $D$  accept only  $\hat{x}'$  that are in the support of class  $y$ . The loss  $L_{D\hat{x}'}$  should have a smaller weight than  $L_{Dx}$  so that, if  $G$  is generating perfect modifications,  $D$  can still know what the support of  $y$  is. Finally, we define the term

$$L_{RegG} = \frac{\|\widehat{\Delta x}\|_2}{\sqrt{n}}, \quad (8)$$

where  $n$  is the dimensionality of  $x$ . This penalty is used to enforce that the modified image is the closest point in the learned support of the other class. The final optimization is given by

$$G^* = \underset{G}{\operatorname{argmin}}(\lambda_G L_G + \lambda_{RegG} L_{RegG}), D^* = \underset{D}{\operatorname{argmin}}(\lambda_{Dx} L_{Dx} + \lambda_{D\hat{x}'} L_{D\hat{x}'}), \quad (9)$$

where  $\lambda_G, \lambda_{RegG}, \lambda_{Dx}, \lambda_{D\hat{x}'}$  are hyperparameters.

### 2.3 Adversarial defense and attack

One way to make models more robust is to use adversarial training, which aims to find a robust parameterized classifier  $m$  by optimizing

$$\min_m \max_{\delta} \mathcal{L}(m(x + \delta), y), \|\delta\|_p < \epsilon, \quad (10)$$

where  $\delta$  is a residual with a limited norm,  $\mathcal{L}$  is a classification loss function,  $x$  is an input example and  $y$  its associated ground truth. In PGD [26], the inner maximization is performed using iterative optimization with gradient ascent with  $k$  steps of size  $\eta$ , and, usually,  $p = \infty$ . The method can also be used as a strong adversarial attack.

## 3 Experiments

We empirically analyzed<sup>1</sup> if improving the robustness of a model using PGD training increased its alignment  $\overline{\alpha_{\Delta x}}$ , and if increasing  $\overline{\alpha_{\Delta x}}$  by using the alignment penalty  $L_\alpha$  improved the model robustness. We compared both training methods against a baseline using plain supervised learning. We also compared the values given by our metric  $\overline{\alpha_{\Delta x}}$  against values given by the metric proposed by Etmann et al. [8], to which we refer as  $\overline{\alpha_x}$ . We adapted the metric, adding a normalization by  $\|x\|_2$  to change the range of values to  $[0, 1]$ , to allow a comparison with  $\alpha_{\Delta x}$ . The metric was modified as

$$\overline{\alpha_x} = \int P(x) \frac{|\langle x, \nabla L(x) \rangle|}{\|x\|_2 \|\nabla L(x)\|_2} dx. \quad (11)$$

All experiments were performed five times. We report the average resulting values and their standard deviations. Section A of the Supplementary Material presents details about the experimental setup.

### 3.1 Datasets

We performed evaluations on four datasets, two of which were synthetic datasets for which we could define the correct  $\Delta x$ . For the *Spheres* dataset, defined in Section 2.1, samples were always drawn randomly at runtime from a standard Gaussian distribution and normalized to the radius of the respective class. The correct  $\Delta x$  was calculated by

$$\Delta x = \begin{cases} 0.3 x, & \text{if } \|x\| = 1 \\ -0.3 \frac{x}{1.3}, & \text{if } \|x\| = 1.3 \end{cases}. \quad (12)$$

We created another synthetic dataset, which we refer to as *Squares*, composed of images with  $224 \times 224$  pixels of centered large or small squares, with sides of 142 and 88 pixels, respectively. To make the images unique, spatially smoothed Gaussian noise was randomly sampled for each image

<sup>1</sup>PyTorch code is available at <https://github.com/ricbl/gradiant-direction-of-robust-models>

Table 1: Examples of measures for generated  $\widehat{\Delta x}$  for the *Spheres* datasets, for two random samples.

Class	$\ x\ _2$	$\ \widehat{\Delta x}\ _2$	$\ \Delta x\ _2$	$\ \hat{x}'\ _2$	$\ x'\ _2$	$\text{sim}(\Delta x, \widehat{\Delta x})$
0	1.0	.307	.3	1.27	1.3	.858
1	1.3	.360	.3	0.99	1.0	.898

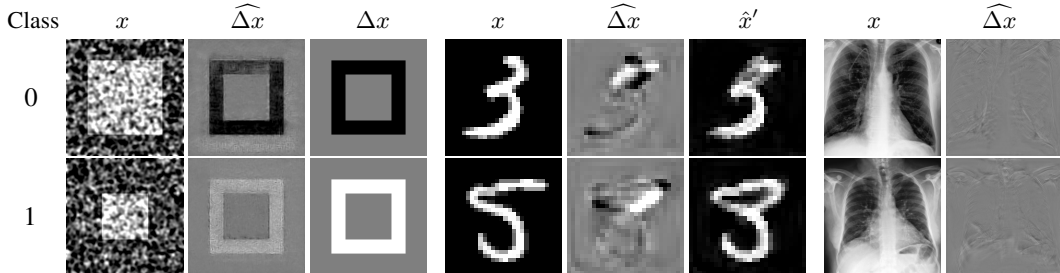


Figure 2: Results of the generated  $\widehat{\Delta x}$  for random samples in the image datasets. The  $x'$  column is suppressed for the *COPD* dataset because of its resemblance to  $x$ .

and added to it. The correct gradient was calculated using the subtraction of a noiseless image of the current square from a noiseless image of a square of the opposite class.

To check if the results hold for more complex datasets, we used the MNIST [24] dataset and a private chest x-ray (CXR) dataset, which we will refer to as *COPD*. To change the MNIST dataset to a binary class formulation, we used only two similar digits, 3 and 5. A fixed set of 10% of the training set was used for validation, and the range, similarly to all other image datasets, was adjusted to  $[-1, 1]$ . The *COPD* dataset contained posterioranterior (PA) CXRs labeled for chronic obstructive pulmonary disease (COPD) using pulmonary function tests (PFTs) [19]. For both datasets, the method presented in Section 2.2 was used to estimate the correct gradient. More details about the datasets are given in the Supplementary Material, and example images can be seen in Figure 2.

### 3.2 Validating gradient estimation

To validate the method for estimating  $\Delta x$ , we applied it to both datasets for which we know the correct  $\Delta x$  and measured the alignment between  $\Delta x$  and  $\widehat{\Delta x}$ . We found that, for the *Spheres* dataset,  $\text{sim}(\Delta x, \widehat{\Delta x}) = 0.874 \pm 0.019$ , and, for the *Squares* dataset,  $\text{sim}(\Delta x, \widehat{\Delta x}) = 0.893 \pm 0.058$ , which demonstrates close alignment for both datasets. Table 1 shows examples of results for the *Spheres* dataset. Figure 2 shows examples of generated  $\widehat{\Delta x}$  for all the image datasets. The generated  $\widehat{\Delta x}$  were similar to the expected  $\Delta x$  for the *Spheres* and the *Squares* datasets. For the MNIST dataset, the generated  $\hat{x}'$  resembled digits of the opposite class and were almost ambiguous. This ambiguity is expected when finding the closest point in the support of the opposite class. For the *COPD* dataset,  $\widehat{\Delta x}$  had small norms, highlighting mainly areas around the diaphragms and the upper lungs. Diaphragm shape and position are used as COPD evidence in CXR [9]. The small norms are likely due to the continuous characteristic of disease severity, which leads to the support of both classes being on the same manifold. Furthermore, most samples had PFT values close to the defined threshold between classes. Consequently, most samples were probably close to the decision boundary.

### 3.3 Alignment and robustness

For the robustness metric, we report the estimated point  $\epsilon_{50\%}$  where 50% of test examples are being classified incorrectly after applying PGD attack with varying values of  $\epsilon$ . We report a single value instead of the usual curve of accuracy as a function of  $\epsilon$  to have a more objective evaluation. We used accuracy as the basis of the metric so that it is comparable to the style of reporting in the literature. The defined  $\epsilon_{50\%}$ , used only for reporting, is equivalent to considering misclassified inputs to have  $\rho(x) = 0$  and calculating the median of the estimated robustness, which has been used to evaluate the baseline metric  $\bar{\alpha}_x$  [8]. In addition to using PGD with  $p = \infty$ , we calculated the robustness of the

Table 2: Results for robustness, alignments, and accuracy after training the models using a plain supervised training baseline (B), alignment penalty ( $L_\alpha$ ), and adversarial training with PGD (P) for 4 datasets: *Spheres* (S), *Squares* (Q), MNIST-3/5 (M), *COPD* (C). Attacks employed to calculate robustness include PGD [26], with two types of norms, and the black-box Square Attack [1] (BIBox).

Setup	Accuracy (%)	$\epsilon_{50\%}$ PGD $_{p=\infty}$	$\epsilon_{50\%}$ PGD $_{p=2}$	$\epsilon_{50\%}$ BIBox $_{p=\infty}$	$\overline{\alpha_{\Delta x}}$ (ours)	$\overline{\alpha_x}$
S-B	99.4±0.8	0.0058±.0001	.099±.009	0.0063±.0004	.659±.028	.659±.028
S- $L_\alpha$	100.±0.0	0.0076±.0002	.133±.001	0.0083±.0003	.886±.002	.886±.002
S-P	100.±0.0	0.0073±.0001	.126±.002	0.0080±.0001	.851±.001	.851±.001
Q-B	100.±0.0	0.031±.008	16.5±1.6	0.170±.041	.026±.007	.022±.006
Q- $L_\alpha$	100.±0.0	0.435±.061	61.9±5.4	0.405±.001	.926±.004	.357±.009
Q-P	100.±0.0	0.501±.030	61.3±2.0	0.337±.011	.222±.042	.151±.051
M-B	99.3±0.4	0.198±.012	2.23±.01	0.232±.010	.171±.029	.013±.003
M- $L_\alpha$	99.5±0.5	0.357±.011	3.88±.08	0.351±.009	.678±.078	.196±.010
M-P	99.5±0.2	0.547±.007	4.20±.15	0.495±.005	.345±.018	.040±.032
C-B	66.3±1.5	0.006±.0021	0.73±.33	0.021±.0063	.016±.005	.002±.0003
C- $L_\alpha$	64.2±5.4	0.020±.0047	2.91±.65	0.028±.0074	.163±.009	.064±.019
C-P	64.7±2.7	0.063±.0294	4.97±2.4	0.072±.0324	.081±.007	.023±.013

models against  $L^2$ -constrained PGD attacks, with an adapted step  $\eta_{L^2} = \eta_{L^\infty} \times \sqrt{n}$ , where  $n$  is the dimensionality of the data, and against Square Attack [1], an iterative black-box attack. Since the Square Attack is formulated for images, we adapt it to the *Spheres* dataset by reshaping its 500-feature vectors to a  $20 \times 25$  image. We used the black-box attack to evaluate if any of the defenses were causing gradient obfuscation [2]. For the MNIST and the *COPD* datasets, training with alignment penalty as defined in (5) employed a different  $G$  for each run, and  $\overline{\alpha_{\Delta x}}$  was calculated using one of the other four trained  $G$ . Results for robustness and alignment are given in Table 2. The graphs of accuracy as a function of perturbation norm are given in Section B in the Supplementary Material.

The alignment  $\overline{\alpha_{\Delta x}}$  increased for all PGD-trained models when compared to baseline. Similarly, the robustness of all models trained with the  $L_\alpha$  penalty increased when compared to the baseline. These results show that alignment and robustness are closely related, and one is a consequence of the other. Theoretically, for the *Spheres* dataset,  $\rho_x / \overline{\alpha_{\Delta x}} = 0.15$  when  $p = 2$ . This value is close to the ratio of values in Table 2, which lies between 0.148 and 0.151, experimentally validating the results from the theoretical analysis. For the other datasets, even though the penalty alignment training had the closest alignment, PGD had the highest robustness when  $p = \infty$ . PGD likely not only aligns the gradient, but also improves robustness in other ways, such as providing a denser sampling of inputs, especially in critical regions, and making the model more locally linear [28]. In Table 2, only models trained using PGD exhibited signs gradient obfuscation, highlighted by the black-box attack being considerably more potent than the PGD attack for some datasets. Section B in the Supplementary Material provides an analysis of gradient obfuscation using the graphs of accuracy as a function of perturbation norm.

Except for the *Spheres* dataset, where our proposed alignment metrics  $\alpha_{\Delta x}$  mathematically reduces to the alignment metric  $\alpha_x$  [8], our metric  $\overline{\alpha_{\Delta x}}$  was larger than  $\overline{\alpha_x}$  in all cases, demonstrating that robust models are more closely aligned with  $\Delta x$  than with  $x$ . In some cases, neither metric had its highest value for the most robust model. It is also worth noting that  $\overline{\alpha_{\Delta x}}$  employs the direction to which the gradient is pointing, providing more information than the  $\overline{\alpha_x}$  metric, which has an absolute value in its numerator.

Figure 3 shows  $\nabla_{L(x)}$  for random images in each dataset for all three training methods. The saliency maps are noisier for the baseline and smoother for models trained with  $L_\alpha$ , whereas PGD-trained models have an intermediate amount of noise and are more localized. These observations confirm that robust models provide more meaningful saliency maps, in comparison to the baseline.



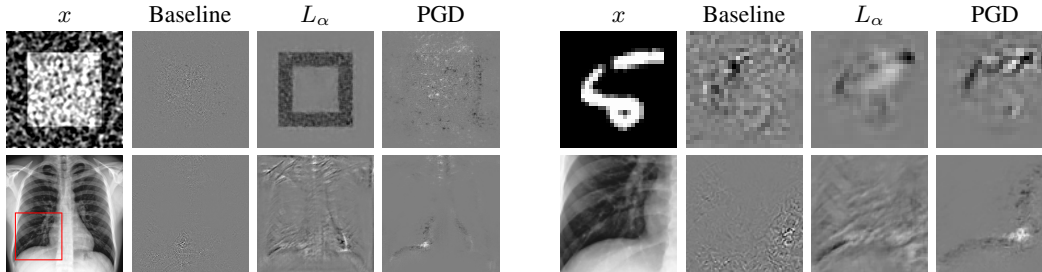


Figure 3: Examples of the saliency map  $\nabla_{L(x)}$  for all the training methods. Bottom right: details of the saliency maps for the *COPD* dataset for the region defined by the red square.

## 4 Conclusion and future work

We proposed a novel method for measuring alignment between the gradient of robust models and interpretable directions by using the concept of cosine similarity between gradient and the vector pointing to the closest example of the support of the opposite class. We validated the proposed metric theoretically and showed experimentally that alignment increases with PGD training and that robustness increases with alignment enforcement. Trained models also showed a closer alignment with the proposed metric than with another metric definition. The metric was not directly predictive of robustness since models with the strongest alignment were not always the most robust. This finding is possibly a result of the violation of the strong assumptions of the theoretical analysis. It also highlights the possibility of PGD increasing robustness by means other than gradient alignment. Finally, we expand our fundamental understanding of adversarial defenses, benefiting future analyses of model robustness.

One possible future line of work is the study of feasibility of applying the proposed techniques to multi-class tasks. This work will require tackling the practical obstacles due to the increased complexity in the generative part of the technique. Combining the proposed method with PGD and with LLR is another direction for future work.

## References

- [1] Maksym Andriushchenko, Francesco Croce, Nicolas Flammarion, and Matthias Hein. Square attack: a query-efficient black-box adversarial attack via random search. In *Proceedings of the European Conference on Computer Vision (ECCV)*, 2020.
- [2] Anish Athalye, Nicholas Carlini, and David A. Wagner. Obfuscated gradients give a false sense of security: Circumventing defenses to adversarial examples. In Jennifer G. Dy and Andreas Krause, editors, *Proceedings of the 35th International Conference on Machine Learning, ICML 2018, Stockholmsmässan, Stockholm, Sweden, July 10-15, 2018*, volume 80 of *Proceedings of Machine Learning Research*, pages 274–283. PMLR, 2018. URL <http://proceedings.mlr.press/v80/athalye18a.html>.
- [3] Nicholas Carlini and David A. Wagner. Adversarial examples are not easily detected: Bypassing ten detection methods. In Bhavani M. Thuraisingham, Battista Biggio, David Mandell Freeman, Brad Miller, and Arunesh Sinha, editors, *Proceedings of the 10th ACM Workshop on Artificial Intelligence and Security, AISec@CCS 2017, Dallas, TX, USA, November 3, 2017*, pages 3–14. ACM, 2017. doi: 10.1145/3128572.3140444. URL <https://doi.org/10.1145/3128572.3140444>.
- [4] Nicholas Carlini, Guy Katz, Clark W. Barrett, and David L. Dill. Ground-truth adversarial examples. *CoRR*, abs/1709.10207, 2017. URL <http://arxiv.org/abs/1709.10207>.
- [5] Alvin Chan, Yi Tay, and Yew-Soon Ong. What it thinks is important is important: Robustness transfers through input gradients. *CoRR*, abs/1912.05699, 2019. URL <http://arxiv.org/abs/1912.05699>.
- [6] Alvin Chan, Yi Tay, Yew-Soon Ong, and Jie Fu. Jacobian adversarially regularized networks for robustness. In *8th International Conference on Learning Representations, ICLR 2020, Addis Ababa, Ethiopia, April 26-30, 2020*. OpenReview.net, 2020. URL <https://openreview.net/forum?id=Hke0V1rKPS>.
- [7] Harris Drucker and Yann LeCun. Improving generalization performance using double backpropagation. *IEEE Trans. Neural Networks*, 3(6):991–997, 1992. doi: 10.1109/72.165600. URL <https://doi.org/10.1109/72.165600>.

- [8] Christian Etmann, Sebastian Lunz, Peter Maass, and Carola Schönlieb. On the connection between adversarial robustness and saliency map interpretability. In Kamalika Chaudhuri and Ruslan Salakhutdinov, editors, *Proceedings of the 36th International Conference on Machine Learning, ICML 2019, 9-15 June 2019, Long Beach, California, USA*, volume 97 of *Proceedings of Machine Learning Research*, pages 1823–1832. PMLR, 2019. URL <http://proceedings.mlr.press/v97/etmann19a.html>.
- [9] WL Foster Jr, EI Gimenez, MA Roubidoux, RH Sherrier, RH Shannon, VL Roggli, and PC Pratt. The emphysemas: radiologic-pathologic correlations. *Radiographics*, 13(2):311–328, 1993.
- [10] Justin Gilmer, Luke Metz, Fartash Faghri, Samuel S. Schoenholz, Maithra Raghu, Martin Wattenberg, and Ian J. Goodfellow. Adversarial spheres. *CoRR*, abs/1801.02774, 2018. URL <http://arxiv.org/abs/1801.02774>.
- [11] Ian J. Goodfellow, Jean Pouget-Abadie, Mehdi Mirza, Bing Xu, David Warde-Farley, Sherjil Ozair, Aaron C. Courville, and Yoshua Bengio. Generative adversarial nets. In Zoubin Ghahramani, Max Welling, Corinna Cortes, Neil D. Lawrence, and Kilian Q. Weinberger, editors, *Advances in Neural Information Processing Systems 27: Annual Conference on Neural Information Processing Systems 2014, December 8-13 2014, Montreal, Quebec, Canada*, pages 2672–2680, 2014. URL <http://papers.nips.cc/paper/5423-generative-adversarial-nets>.
- [12] Ian J. Goodfellow, Jonathon Shlens, and Christian Szegedy. Explaining and harnessing adversarial examples. In Yoshua Bengio and Yann LeCun, editors, *3rd International Conference on Learning Representations, ICLR 2015, San Diego, CA, USA, May 7-9, 2015, Conference Track Proceedings*, 2015. URL <http://arxiv.org/abs/1412.6572>.
- [13] Chuan Guo, Mayank Rana, Moustapha Cissé, and Laurens van der Maaten. Countering adversarial images using input transformations. In *6th International Conference on Learning Representations, ICLR 2018, Vancouver, BC, Canada, April 30 - May 3, 2018, Conference Track Proceedings*. OpenReview.net, 2018. URL <https://openreview.net/forum?id=SyJ7C1WCb>.
- [14] Kaiming He, Xiangyu Zhang, Shaoqing Ren, and Jian Sun. Deep residual learning for image recognition. In *2016 IEEE Conference on Computer Vision and Pattern Recognition, CVPR 2016, Las Vegas, NV, USA, June 27-30, 2016*, pages 770–778. IEEE Computer Society, 2016. doi: 10.1109/CVPR.2016.90. URL <https://doi.org/10.1109/CVPR.2016.90>.
- [15] Matthias Hein and Maksym Andriushchenko. Formal guarantees on the robustness of a classifier against adversarial manipulation. In Isabelle Guyon, Ulrike von Luxburg, Samy Bengio, Hanna M. Wallach, Rob Fergus, S. V. N. Vishwanathan, and Roman Garnett, editors, *Advances in Neural Information Processing Systems 30: Annual Conference on Neural Information Processing Systems 2017, 4-9 December 2017, Long Beach, CA, USA*, pages 2266–2276, 2017.
- [16] Andrew Ilyas, Shibani Santurkar, Dimitris Tsipras, Logan Engstrom, Brandon Tran, and Aleksander Madry. Adversarial examples are not bugs, they are features. In Hanna M. Wallach, Hugo Larochelle, Alina Beygelzimer, Florence d’Alché-Buc, Emily B. Fox, and Roman Garnett, editors, *Advances in Neural Information Processing Systems 32: Annual Conference on Neural Information Processing Systems 2019, NeurIPS 2019, 8-14 December 2019, Vancouver, BC, Canada*, pages 125–136, 2019. URL <http://papers.nips.cc/paper/8307-adversarial-examples-are-not-bugs-they-are-features>.
- [17] Sergey Ioffe and Christian Szegedy. Batch normalization: Accelerating deep network training by reducing internal covariate shift. In Francis R. Bach and David M. Blei, editors, *Proceedings of the 32nd International Conference on Machine Learning, ICML 2015, Lille, France, 6-11 July 2015*, volume 37 of *JMLR Workshop and Conference Proceedings*, pages 448–456. JMLR.org, 2015. URL <http://proceedings.mlr.press/v37/ioffe15.html>.
- [18] Daniel Jakubovitz and Raja Giryes. Improving DNN robustness to adversarial attacks using jacobian regularization. In Vittorio Ferrari, Martial Hebert, Cristian Sminchisescu, and Yair Weiss, editors, *Computer Vision - ECCV 2018 - 15th European Conference, Munich, Germany, September 8-14, 2018, Proceedings, Part XII*, volume 11216 of *Lecture Notes in Computer Science*, pages 525–541. Springer, 2018. doi: 10.1007/978-3-030-01258-8\_32. URL [https://doi.org/10.1007/978-3-030-01258-8\\_32](https://doi.org/10.1007/978-3-030-01258-8_32).
- [19] Jeremy Daniel Johnson and Wesley M Theurer. A stepwise approach to the interpretation of pulmonary function tests. *American family physician*, 89 5:359–66, 2014.
- [20] Simran Kaur, Jeremy Cohen, and Zachary C. Lipton. Are perceptually-aligned gradients a general property of robust classifiers? *CoRR*, abs/1910.08640, 2019. URL <http://arxiv.org/abs/1910.08640>.

- [21] Ashkan Khakzar, Shadi Albarqouni, and Nassir Navab. Learning interpretable features via adversarially robust optimization. In Dinggang Shen, Tianming Liu, Terry M. Peters, Lawrence H. Staib, Caroline Essert, Sean Zhou, Pew-Thian Yap, and Ali Khan, editors, *Medical Image Computing and Computer Assisted Intervention - MICCAI 2019 - 22nd International Conference, Shenzhen, China, October 13-17, 2019, Proceedings, Part VI*, volume 11769 of *Lecture Notes in Computer Science*, pages 793–800. Springer, 2019. doi: 10.1007/978-3-030-32226-7\_88. URL [https://doi.org/10.1007/978-3-030-32226-7\\_88](https://doi.org/10.1007/978-3-030-32226-7_88).
- [22] Diederik P. Kingma and Jimmy Ba. Adam: A method for stochastic optimization. In Yoshua Bengio and Yann LeCun, editors, *3rd International Conference on Learning Representations, ICLR 2015, San Diego, CA, USA, May 7-9, 2015, Conference Track Proceedings*, 2015. URL <http://arxiv.org/abs/1412.6980>.
- [23] Ricardo Bigolin Lanfredi, Joyce D. Schroeder, Clement Vachet, and Tolga Tasdizen. Adversarial regression training for visualizing the progression of chronic obstructive pulmonary disease with chest x-rays. In Dinggang Shen, Tianming Liu, Terry M. Peters, Lawrence H. Staib, Caroline Essert, Sean Zhou, Pew-Thian Yap, and Ali Khan, editors, *Medical Image Computing and Computer Assisted Intervention - MICCAI 2019 - 22nd International Conference, Shenzhen, China, October 13-17, 2019, Proceedings, Part VI*, volume 11769 of *Lecture Notes in Computer Science*, pages 685–693. Springer, 2019. doi: 10.1007/978-3-030-32226-7\_76. URL [https://doi.org/10.1007/978-3-030-32226-7\\_76](https://doi.org/10.1007/978-3-030-32226-7_76).
- [24] Y. Lecun, L. Bottou, Y. Bengio, and P. Haffner. Gradient-based learning applied to document recognition. *Proceedings of the IEEE*, 86(11):2278–2324, 1998.
- [25] Chunchuan Lyu, Kaizhu Huang, and Hai-Ning Liang. A unified gradient regularization family for adversarial examples. In Charu C. Aggarwal, Zhi-Hua Zhou, Alexander Tuzhilin, Hui Xiong, and Xindong Wu, editors, *2015 IEEE International Conference on Data Mining, ICDM 2015, Atlantic City, NJ, USA, November 14-17, 2015*, pages 301–309. IEEE Computer Society, 2015. doi: 10.1109/ICDM.2015.84. URL <https://doi.org/10.1109/ICDM.2015.84>.
- [26] Aleksander Madry, Aleksandar Makelov, Ludwig Schmidt, Dimitris Tsipras, and Adrian Vladu. Towards deep learning models resistant to adversarial attacks. In *6th International Conference on Learning Representations, ICLR 2018, Vancouver, BC, Canada, April 30 - May 3, 2018, Conference Track Proceedings*. OpenReview.net, 2018. URL <https://openreview.net/forum?id=rJzIBfZAb>.
- [27] Adam Noack, Isaac Ahern, Dejing Dou, and Boyang Li. Does interpretability of neural networks imply adversarial robustness? *CoRR*, abs/1912.03430, 2019. URL <http://arxiv.org/abs/1912.03430>.
- [28] Chongli Qin, James Martens, Sven Gowal, Dilip Krishnan, Krishnamurthy Dvijotham, Alhussein Fawzi, Soham De, Robert Stanforth, and Pushmeet Kohli. Adversarial robustness through local linearization. In Hanna M. Wallach, Hugo Larochelle, Alina Beygelzimer, Florence d’Alché-Buc, Emily B. Fox, and Roman Garnett, editors, *Advances in Neural Information Processing Systems 32: Annual Conference on Neural Information Processing Systems 2019, NeurIPS 2019, 8-14 December 2019, Vancouver, BC, Canada*, pages 13824–13833, 2019. URL <http://papers.nips.cc/paper/9534-adversarial-robustness-through-local-linearization>.
- [29] Olaf Ronneberger, Philipp Fischer, and Thomas Brox. U-net: Convolutional networks for biomedical image segmentation. In Nassir Navab, Joachim Hornegger, William M. Wells III, and Alejandro F. Frangi, editors, *Medical Image Computing and Computer-Assisted Intervention - MICCAI 2015 - 18th International Conference Munich, Germany, October 5 - 9, 2015, Proceedings, Part III*, volume 9351 of *Lecture Notes in Computer Science*, pages 234–241. Springer, 2015. doi: 10.1007/978-3-319-24574-4\_28. URL [https://doi.org/10.1007/978-3-319-24574-4\\_28](https://doi.org/10.1007/978-3-319-24574-4_28).
- [30] Andrew Slavin Ross and Finale Doshi-Velez. Improving the adversarial robustness and interpretability of deep neural networks by regularizing their input gradients. In Sheila A. McIlraith and Kilian Q. Weinberger, editors, *Proceedings of the Thirty-Second AAAI Conference on Artificial Intelligence (AAAI-18), the 30th innovative Applications of Artificial Intelligence (IAAI-18), and the 8th AAAI Symposium on Educational Advances in Artificial Intelligence (EAAI-18), New Orleans, Louisiana, USA, February 2-7, 2018*, pages 1660–1669. AAAI Press, 2018. URL <https://www.aaai.org/ocs/index.php/AAAI/AAAI18/paper/view/17337>.
- [31] Daniel Smilkov, Nikhil Thorat, Been Kim, Fernanda B. Viégas, and Martin Wattenberg. Smoothgrad: removing noise by adding noise. *CoRR*, abs/1706.03825, 2017. URL <http://arxiv.org/abs/1706.03825>.
- [32] Thomas Tanay and Lewis D. Griffin. A boundary tilting perspective on the phenomenon of adversarial examples. *CoRR*, abs/1608.07690, 2016. URL <http://arxiv.org/abs/1608.07690>.

- [33] Dimitris Tsipras, Shibani Santurkar, Logan Engstrom, Alexander Turner, and Aleksander Madry. Robustness may be at odds with accuracy. In *7th International Conference on Learning Representations, ICLR 2019, New Orleans, LA, USA, May 6-9, 2019*. OpenReview.net, 2019. URL <https://openreview.net/forum?id=SyxAb30cY7>.
- [34] Tsui-Wei Weng, Huan Zhang, Pin-Yu Chen, Jinfeng Yi, Dong Su, Yupeng Gao, Cho-Jui Hsieh, and Luca Daniel. Evaluating the robustness of neural networks: An extreme value theory approach. In *6th International Conference on Learning Representations, ICLR 2018, Vancouver, BC, Canada, April 30 - May 3, 2018, Conference Track Proceedings*. OpenReview.net, 2018. URL <https://openreview.net/forum?id=BkUH1MZ0b>.
- [35] Walt Woods, Jack Chen, and Christof Teuscher. Adversarial explanations for understanding image classification decisions and improved neural network robustness. *Nature Machine Intelligence*, 1(11): 508–516, 2019.
- [36] Han Xu, Yao Ma, Haochen Liu, Debayan Deb, Hui Liu, Jiliang Tang, and Anil K. Jain. Adversarial attacks and defenses in images, graphs and text: A review. *CoRR*, abs/1909.08072, 2019. URL <http://arxiv.org/abs/1909.08072>.

## Supplementary Material

### A Experimental setup and dataset details

Table 3: Details about datasets and training setup

<i>Properties &amp; Hyperparameters</i> \ <i>Dataset</i>	<i>Spheres</i>	<i>Squares</i>	MNIST	<i>COPD</i>
Train set size	10,000,000/epoch	10,000	10,397	3,711
Validation set size	200	200	1,155	596
Test set size	1,000	1,000	1,902	950
Data dimensionality	500	224×224	28×28	224×224
% of samples of class 0 - training set	~50%	49.7%	53.1%	63%
% of samples of class 0 - validation set	~50%	53.0%	53.1%	49.8%
% of samples of class 0 - test set	~50%	49.5%	53.1%	58.2%
PGD - $\epsilon$ for training	0.005	0.2	0.3	0.006
PGD - $\eta$	0.002	0.02	0.02	0.02
# epochs	80	30	30	30
$\lambda_\alpha$	0.1	0.1	0.1	10
Batch size	50	12	12	12
Average training time - baseline (hours)	2.3	1.3	4.1	3.7
Average training time - $G$ (hours)	3	0.8	0.1	1
Average training time - $L_\alpha$ (hours)	6.2	1.5	3.7	4.2
Average training time - PGD (hours)	15.4	2.5	3.1	4.9
Average test time - Square Attack (hours)	0.3	6.3	8.8	3.8

For the *Spheres* dataset, we used a 2-hidden layer network, with 1000 neurons per layer, batch normalization [17], and ReLU non-linearity, varying the output of the last layer to 500 for the generator and 1 for the classifiers. For all other datasets, we used a Resnet-18 [14] as the classifier and U-net [29] as the generator. In the U-net, we utilized two levels of downsampling for MNIST and four levels of downsampling for *Squares* and *COPD*. The values of  $\neg y$  and  $y$  were concatenated as channels to the U-net’s bottleneck. PGD attacks, for training and validation, used  $k = 40$ . The Square Attack was used with 5000 queries per attack and 80% as an initial percentage of features to be modified. We used the Adam optimizer [22] with a learning rate of  $10^{-4}$ . For training  $G$ , we used  $\lambda_G = 0.3$ ,  $\lambda_{RegG} = 0.5$ ,  $\lambda_{D_x} = 1$  and  $\lambda_{D_{\hat{x}}} = 0.01$ . The best epoch was chosen by determining the one with minimal total loss for choosing  $G$  and the highest robustness against PGD ( $p = \infty$ ) on the validation set for classifier models. Further details on hyperparameters specific to each dataset are given in Table 3. The computer infrastructure employed included 11 Titan V, 6 Titan RTX, and 8 Titan V100 SMX2, and all GPUs were used interchangeably depending on availability. Some of the experiments required large GPU memory capacity, which was available only on Titan RTX. Training, combined with best epoch validation, took between 5 minutes and 17 hours for each run, depending on the dataset, method, and GPU used. The average time for method and dataset are reported in Table 3. Test evaluations for PGD attack took less than 20 minutes each. Table 3 also presents further quantitative detail about the datasets used.

The *COPD* dataset was retrospectively gathered in the University of Utah Hospital, and the PFTs used for labeling were acquired within 30 days of the CXR. Patients who have undergone lung transplant and patients with several images in the same CXR study were excluded. Patients with an FEV<sub>1</sub>/FVC lower than 0.7 [19] were assigned to class 1 as having COPD. Images were center-cropped, resized to  $256 \times 256$ , cropped to  $224 \times 224$  (randomly in training), and had their histograms equalized and range adjusted to  $[-1, 1]$ . The dataset was split in training, validation, and test sets by patient ID, since some patients were associated with more than one sample.

### B Additional robustness graphs

In Figure 4, all attacks with a large enough bound were able to get 100% success, and increasing the perturbation norm  $\epsilon$  increased attack success rate, signs that gradient does not suffer from intensive gradient obfuscation [2] in any of the methods. For the *Squares* dataset, the alignment penalty training method showed some gradient obfuscation for one of the classes, as seen in the bottom gap between black-box attack and PGD attack in Figure 4, without largely reflecting on the numbers of Table 2.

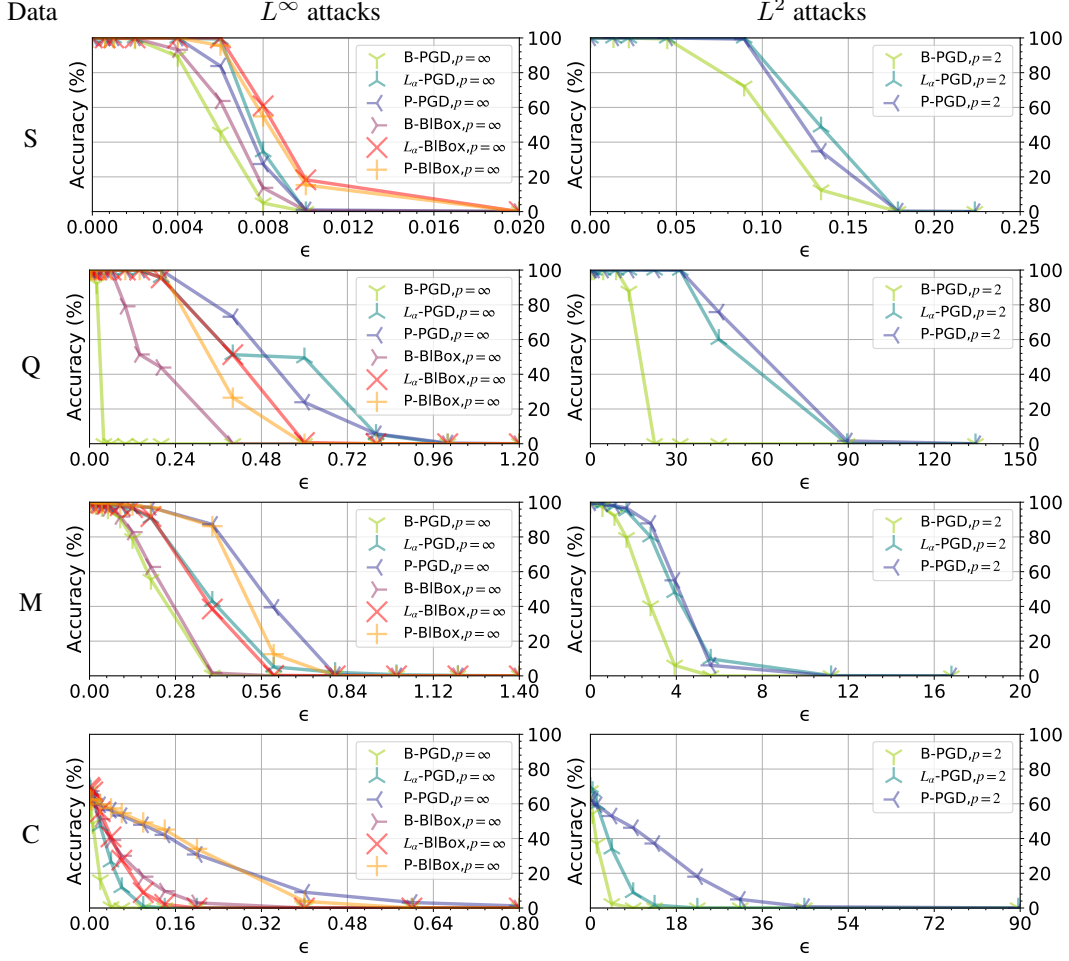


Figure 4: Accuracy of models as a function of perturbation norm after training using a plain supervised training baseline (B), alignment penalty ( $L_\alpha$ ), and adversarial training with PGD (P) for 4 datasets: *Spheres* (S), *Squares* (Q), MNIST-3/5 (M), *COPD* (C). We report results for 3 attacks: PGD [26] restricted by the  $L^\infty$  norm, the black-box Square Attack [1] (BIBox) restricted by the  $L^\infty$  norm, and PGD [26] restricted by the  $L^2$  norm. Models were selected randomly from the 5 trained models for each training setup.

## C Proofs

**Lemma 1.** Let  $l(x) = \sup\{r : \forall v \text{ s.t. } \|x - v\|_2 < r, \exists! w, \exists! b \text{ s.t. } m(v) = \sigma(\langle v, w \rangle + b)\}$ , i.e.  $l(x)$  is the radius of the largest hypersphere around  $x$  where a decision model  $m$  can be defined by a specific linear decision function. Assuming that  $l(x) \geq |\rho(x)|$  for  $m$ , then the logits of  $m$  can be modeled as a linear function, i.e.  $\langle x, w \rangle + b$ , for robustness assessment, resulting in a robustness magnitude in  $x$  given by  $|\rho(x)| = \left| \frac{\langle x, w \rangle + b}{\|w\|_2} \right|$ .

Lemma 1 is a direct consequence of Lemma 1 given in [8], where a proof is presented. We use the term "locally linear around  $x$ " in Theorems 1 and 2 to refer to models that satisfy Lemma 1.

**Theorem 1.** Let  $\text{sim}(u, v)$  be the alignment between vectors  $u$  and  $v$ , defined by their cosine similarity  $\text{sim}(u, v) = \frac{\langle u, v \rangle}{\|u\|_2 \|v\|_2}$ , and let  $m$  be a binary decision model. For a pair of examples  $x_0$  and  $x_1$  from a binary dataset, of class 0 and 1, respectively, and around which  $m$  is locally linear, the combined robustness  $\rho(x_0) + \rho(x_1)$  of  $m$  is directly proportional to  $\alpha$  according to  $\rho(x_0) + \rho(x_1) = \|x_1 - x_0\|_2 \times \alpha$ , where  $\alpha = \text{sim}(x_1 - x_0, \nabla_{L(x_0)}) = \text{sim}(x_0 - x_1, \nabla_{L(x_1)})$  and  $L(x_i)$  is the binary cross-entropy loss for example  $x_i$ .

*Proof.* Since we assume local linearity, the model can be represented by  $m(x) = \sigma(\langle x, w \rangle + b)$  by using Lemma 1. We also note that  $\text{sim}(w, \nabla_{L(x_0)}) = 1$  and  $\text{sim}(w, \nabla_{L(x_1)}) = -1$ . The alignments can be simplified as

$$\alpha_0 = \text{sim}(x_1 - x_0, \nabla_{L(x_0)}) = \text{sim}(x_1 - x_0, w), \quad (13)$$

$$\alpha_1 = \text{sim}(x_0 - x_1, \nabla_{L(x_1)}) = -\text{sim}(x_0 - x_1, w) = \alpha_0 = \alpha, \quad (14)$$

$$\alpha \times \|\Delta x\|_2 = \frac{\langle x_1, w \rangle - \langle x_0, w \rangle}{\|w\|_2}. \quad (15)$$

If  $x$  is correctly classified,  $\rho(x)$  is equal to the distance between  $x$  and the decision boundary. In the case of misclassification, we use the negative of the distance. We can use the equation of distance between  $x$  and the hyperplane defined by  $\langle w, x \rangle + b = 0$  and the result from (15) to get

$$\rho(x_0) = -\frac{\langle x_0, w \rangle + b}{\|w\|_2}, \quad \rho(x_1) = \frac{\langle x_1, w \rangle + b}{\|w\|_2}, \quad (16)$$

$$\rho(x_0) + \rho(x_1) = \frac{\langle x_1, w \rangle - \langle x_0, w \rangle}{\|w\|_2} = \alpha \times \|\Delta x\|_2. \quad (17)$$

□

**Theorem 2.** *Assuming that, for a separable binary dataset, it is possible to define a bijection between the support of both classes  $\text{supp}_0$  and  $\text{supp}_1$  such that, given all bijection pairs  $(x_0, x_1)$ ,  $x_0 \in \text{supp}_0$  and  $x_1 \in \text{supp}_1$ ,*

1.  $P(x_0) = P(x_1)$ ,
2. a binary decision model  $m$  is locally linear around  $x_0$  and  $x_1$ ,

*then the expected robustness of  $m$ ,  $\rho_m$ , is related to the average alignment  $\bar{\alpha}$  between the model gradient with respect to inputs and  $\Delta x$  of pairs  $(x_0, x_1)$ , according to*

$$\rho_m \geq \frac{\inf(K) \times \bar{\alpha}}{2} \quad \text{and} \quad \bar{\alpha} \geq \frac{2 \times \rho_m}{\sup(K)}, \quad (3)$$

*where  $K$  is the set of distances  $\|x_1 - x_0\|_2$  over all pairs  $(x_0, x_1)$ .*

*Proof.* The robustness of a model  $m$  can be written as

$$\rho_m = \int_{\text{supp}_0} P(x) \rho(x) dx + \int_{\text{supp}_1} P(x) \rho(x) dx. \quad (18)$$

Since we can establish a bijection, we can integrate over both supports at the same time, pair by pair of  $x_0$  and  $x_1$ . Since  $P(x_0) = P(x_1)$ , we can factor the probability, resulting in

$$\rho_m = \int_{\text{supp}_0, \text{supp}_1} P(x_0) (\rho(x_0) + \rho(x_1)) dx. \quad (19)$$

It is worth noting that sampling is balanced between the two classes since, from the established bijection,

$$\int_{\text{supp}_0} P(x) dx = \int_{\text{supp}_1} P(x) dx = \frac{1}{2}. \quad (20)$$

Using Theorem 1 to substitute for  $\rho(x_0) + \rho(x_1)$  and using (20),

$$\rho_m = \int_{\text{supp}_0, \text{supp}_1} P(x_0) \alpha_0 \|x_1 - x_0\|_2 dx \geq \frac{\inf(K) \times \bar{\alpha}}{2}, \quad (21)$$

$$\rho_m = \int_{\text{supp}_0, \text{supp}_1} P(x_0) \alpha_0 \|x_1 - x_0\|_2 dx \leq \frac{\text{sup}(K) \times \bar{\alpha}}{2}, \quad \bar{\alpha} \geq \frac{2 \times \rho_m}{\text{sup}(K)}. \quad (22)$$

□